Indian J. pure appl. Math., **11**(11) : 1397-1410, November 1980

BIFURCATION THEORY IN POPULATION MODELS WITH TIME DELAYS

J. N. KAPUR, F.N.A.

Department of Mathematics, Indian Institute of Technology, Kanpur 208016

(*Received* 24 *December* 1979; *after revision* 7 *August* 1980)

The stability of a number of population models with time delays has been examined by separating the regions of stable and unstable equilibrium in the parametric phase space.

1. THE FIRST MODEL

Let $N(t)$ be the population at time t, then the logistic model with discrete time delay is given by

$$dN/dt = N(t)\,[a - bN(t-1)]. \qquad ...(1)$$

Its equilibrium position is given by $\bar{N} = a/b$. Substituting $N(t) = \bar{N} + u(t)$ in (1) and linearizing, we get

$$du/dt = -au(t-1). \qquad ...(2)$$

Trying the solution $u = A \exp(\lambda t)$, we get

$$\lambda + ae^{-\lambda} = 0. \qquad ...(3)$$

(i) Its purely real roots are obtained by solving

$$r + ae^{-r} = 0 \qquad ...(4)$$

which has two real negative roots if $a < e^{-1}$ and two coincident negative roots each equal to (-1) if $a = e^{-1}$.

(ii) Its purely imaginary roots $\pm is$, are obtained by solving

$$a \cos s = 0, \quad s - a \sin s = 0 \qquad ...(5)$$

so that purely imaginary roots occur when

$$a = 2n\pi + \tfrac{1}{2}\pi, \; n = 0, 1, 2, \ldots . \qquad ...(6)$$

(iii) For complex roots $r \pm is$ ($r \neq 0$, $s \neq 0$), we get

$$r + ae^{-r} \cos s = 0, \quad s - ae^{-r} \sin s = 0 \qquad ...(7)$$

or

$$r = -s \cot s, \quad s/a = e^{s \cot s} \sin s. \qquad ...(8)$$

To solve the second eqn. (8), we find the points of intersection of $y = x/a$ and $y = e^{x \cot x} \sin x$. The gragh of the second equation for positive x is given in Fig. 1. It has asymptotes at $x = \pi, 2\pi, 3\pi, 4\pi, \ldots$. The graph has an infinite number of disjoint branches denoted by I, II, III ... .

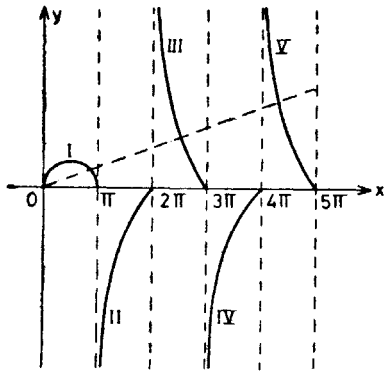

FIG. 1.

The line $y = x/a$ cuts branch I in a unique point for every value of $a > 1/e$. Each point of intersection determines a unique value of s and then the first eqn. (8) determines a unique value for r which is negative if $0 \leqslant s < \pi/2$ and is positive if $\pi/2 < s < \pi$.

Thus corresponding to each value of $a > e^{-1}$, a unique pair of complex roots is determined by the point of intersection of $y = x/a$ with the branch I. Similarly for each value of $a > 0$, there is a unique pair of complex roots determined by the point of intersection of $y = x/a$ with each of the branches III, V, VII, ...

Thus for each value of a, we have an infinite number of complex roots. From eqns. (8)

$$r = -s \cot s,\ a = e^{-s \cot s} \frac{s}{\sin s}. \qquad \ldots(9)$$

Differentiating

$$\frac{dr}{da} = \frac{e^{s \cot s} \sin s\,[s - \sin s \cos s]}{(s - \sin s \cos s)^2 + \sin^4 s}. \qquad \ldots(10)$$

It is easily seen that for s lying between 0 and π, 2π and 3π, 4π and 5π etc., dr/ds, da/ds, dr/da are all positive, so that the real part of each of the infinite number of complex roots increases as a increases. Also

$$\left(\frac{dr}{da}\right)_{2n\pi+(\pi/2)} = \frac{2n\pi + \frac{1}{2}\pi}{(2n\pi + \frac{1}{2}\pi)^2 + 1} \qquad \ldots(11)$$

which decreases fast as n decreases. Table I gives the values of s, r, a for branches I, III and V.

The graphs of the real parts of the roots against a are given in Fig. 2. A and B are the graphs of the real roots and C, D, E are the graphs of roots corresponding to branches I, III and V ... .

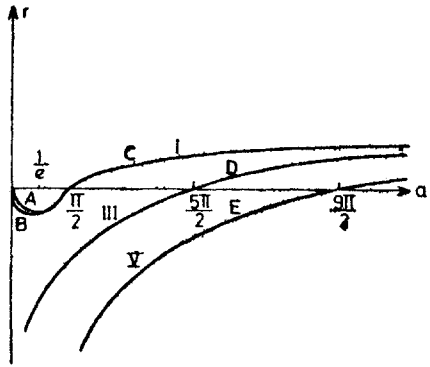

FIG. 2.

TABLE I

	s	0	$\pi/10$	$2\pi/10$	$3\pi/10$	$4\pi/10$	$5\pi/10$	$6\pi/10$	$7\pi/10$	$8\pi/10$
I	r	-1	-0.967	-0.865	-0.685	-0.408	0	0.512	1.598	3.459
	a	e^{-1}	0.387	0.450	0.587	0.878	1.571	3.657	13.433	135.939
	s		$21\pi/10$	$22\pi/10$	$23\pi/10$	$24\pi/10$	$25\pi/10$	$26\pi/10$	$27\pi/10$	
III	r		-20.303	-9.513	-5.250	-2.450	0	2.654	6.163	
	a		0	0.001	0.047	0.684	7.854	122.048	4977.437	
	s		$41\pi/10$	$42\pi/10$	$43\pi/10$	$44\pi/10$	$45\pi/10$	$46\pi/10$		
V	r		-39.642	-18.161	-9.615	-4.49	0	4.676		
	a		0	0	0.001	0.0163	14.137	1663.190		

For any given a, the first branch gives the maximum value of the positive r and gives the maximum value in magnitude for negative r.

The signs of the real parts of the roots are given in Fig. 3.

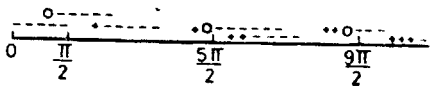

FIG. 3.

When $0 < a < \pi/2$, real parts of all roots are negative.

When $a = \pi/2$, real parts of one pair of roots is zero and real parts of all other complex roots is negative.

When $\pi/2 < a < 5\pi/2$, real parts of one pair of roots are positive and real parts of all other complex roots are negative, and so on.

Just before $a = 2n\pi + \frac{1}{2}\pi$, n pairs of real roots have positive real parts and just after this value, $n + 1$ pairs have positive real parts. At each of the points $2n\pi + \frac{1}{2}\pi$, one pair of complex roots changes the sign of its real parts from negative to positive.

The equilibrium is stable when $a < \pi/2$ and is unstable when $a > \pi/2$. The regions of stable and unstable equilibrium are given by Fig. 4

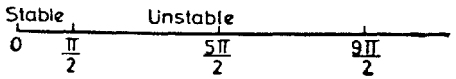

FIG. 4.

2. THE SECOND MODEL

We consider the model

$$\frac{dN}{dt} = N(t)\,[a - bN(t) - cN(t-1)] \qquad \ldots(12)$$

so that there is both a logistic non-delay and a logistic delay term. For this model

$$\bar{N} = \frac{a}{b+c}, \quad \frac{du}{dt} = -\frac{a}{b+c}\,[bu(t) + cu(t-1)] \qquad \ldots(13)$$

$$\lambda + \frac{ab}{b+c} + \frac{ac}{b+c}\,e^{-\lambda} = 0, \quad \lambda + K_1 + K_2 e^{-\lambda} = 0 \qquad \ldots(14)$$

where

$$K_1 = \frac{ab}{b+c}, \quad K_2 = \frac{ac}{b+a}. \qquad \ldots(15)$$

For the purely imaginary roots of (4), we have

$$s - K_2 \sin s = 0, \quad K_1 + K_2 \cos s = 0 \qquad \ldots(16)$$

or

$$K_1 = -s \cot s, \quad K_2 = \frac{s}{\sin s}. \qquad \ldots(17)$$

The parametric phase plane graphs are given in Fig. 5 which also gives the signs of the real parts of the roots in the various regions of the first quadrant of the phase plane. In drawing the graphs, we have used the fact that K_1 and K_2 are essentially positive.

	s	$6\pi/12$	$7\pi/12$	$8\pi/12$	$9\pi/12$	$10\pi/12$	$11\pi/12$
I	K_1	0	0.4910	1.2092	2.3562	4.5345	10.7475
	K_2	1.5908	1.8972	2.4084	3.3522	5.2360	11.1267
	s	$30\pi/12$	$31\pi/12$	$32\pi/12$	$33\pi/12$	$34\pi/12$	$35\pi/12$
II	K_1	0	2.1746	4.8368	8.6394	15.4173	34.1967
	K_2	7.8540	8.4021	9.6736	12.2179	17.8024	35.4031
	s	$54\pi/12$	$55\pi/12$	$56\pi/12$	$57\pi/12$	$58\pi/12$	$59\pi/12$
III	K_1	0	3.8582	8.4644	14.9226	26.3001	57.6459
	K_2	14.1372	14.9067	19.9289	21.1037	30.3687	59.6795

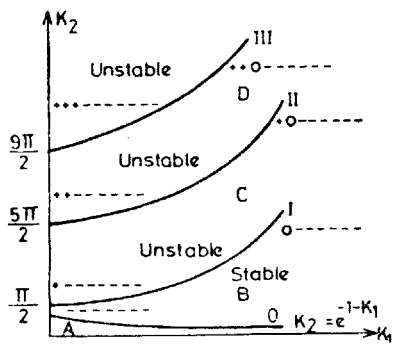

FIG. 5.

We may note that the bifurcation points on the K_2-axis correspond to the bifurcation points in Fig. 4 and the curves on Fig. 5 start with these as base points.

The curves all appear concave upwards. To see this, we note that for the ranges of s considered

$$x = -s \cot s, \; y = \frac{s}{\sin s}, \; \frac{dy}{dx} = \frac{\sin s - s \cos s}{s - \sin s \cos s} > 0 \qquad \ldots(18)$$

$$\frac{d^2y}{dx^2} = \frac{s^2 \sin s + s \sin^2 s \cos s - 2 \sin^3 s}{(s - \sin s \cos s)^2} > 0. \qquad \ldots(19)$$

Equation (14) can be written as

$$z + K_2 e^{K_1} e^{-z} = 0, z = \lambda + K_1. \qquad ...(20)$$

It will have two real roots if

$$K_2 e^{K_1} < e^{-1} \quad \text{or} \quad K_2 < e^{-1-K_1}. \qquad ...(21)$$

When $K_2 = e^{-1-K_1}$, the two roots will coincide and each value of λ will be $-1 - K_1$.

We can now plot the real parts of the roots of (14) against K_1, K_2.

When K_1, K_2 lies in the region A, we get two surfaces below the K_1–K_2 plane. When $K_2 = 0$ i.e. for points on the K_1-axis, for both surfaces $r = -K_1$ and when $K_2 = e^{-1-K_1}$ i.e. for points on the curve 0, $r = -1 - K_1$. The two surfaces are bounded by the curves

$$K_2 = 0, r = -K_1; K_2 = e^{-1-K_1}, r = -1 - K_1. \qquad ...(22)$$

All other roots are complex and the real part of each root determines a surface for r. For the first root the surface starts from the second curve of (27), remains below the K_1–K_2 plane when K_1, K_2 lies in region B and intersects the K_1–K_2 plane along the curve I and then emerges above the plane and thereafter always remains above this plane. The surface corresponding to the real part of the second pair of complex roots remains below the K_1–K_2 plane when K_1–K_2 lies in regions A, B and C, meets the K_1–K_2 plane in curve II and when K_1–K_2 lies in regions D, E, F, ... the surface is above the K_1–K_2 plane. Thus corresponding to the infinity of complex pairs of roots, we get an infinity of surfaces starting from below the K_1–K_2 plane, intersecting it in curves I, II, III, ... and then emerging and remaining above the plane. For any K_1, K_2, the positive value of r given by the first surface will be highest and the negative value of r will go on increasing in magnitude for the different surfaces.

3. The Third Model

We consider the model

$$\frac{dN}{dt} = N(t)\,[a - bN(t) - cN(t-1) - dN(t-2)]. \qquad ...(23)$$

The characteristic equation is

$$\lambda + \bar{K}_1 + \bar{K}_2 e^{-\lambda} + \bar{K}_3 e^{-2\lambda} = 0 \qquad ...(24)$$

where

$$\bar{K}_1 = \frac{ab}{b+c+d}, \quad \bar{K}_2 = \frac{ac}{b+c+d}, \quad \bar{K}_3 = \frac{ad}{b+c+d}. \qquad ...(25)$$

Its purely imaginary roots are given by

$$s - \bar{K}_2 \sin s - \bar{K}_3 \sin 2s = 0, \quad \bar{K}_1 + \bar{K}_2 \cos s + \bar{K}_3 \cos 2s = 0. \quad \ldots(26)$$

For each value of s, it represents a straight line in the $\bar{K}_1$–$\bar{K}_2$–$\bar{K}_3$ phase space so that by eliminating s, we get a family of ruled surfaces. The section of these surfaces by $\bar{K}_3 = 0$ plane are the curves given in Fig. 4.

The equation of the ruled surface can be written as

$$\bar{K}_1 = -s \cot s + t, \quad \bar{K}_2 = \frac{s}{\sin s} - 2 \cos st, \quad \bar{K}_3 = t. \quad \ldots(27)$$

This gives positive values for $\bar{K}_1$, $\bar{K}_2$, $\bar{K}_3$ when

(a) $$s \cot s < t < \frac{s}{\sin 2s}, \quad \pi/4 \leqslant s < \pi/2 \quad \ldots(28)$$

(b) $$\pi/2 \leqslant s < \pi, \quad t > 0. \quad \ldots(29)$$

One branch of the ruled surface is shown in Fig. 6.

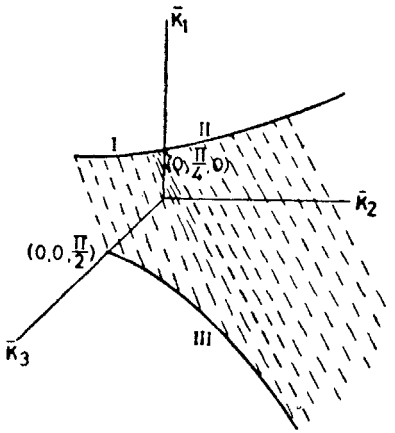

FIG. 6.

The points of the set (a) are the points on the straight lines joining points on curves I and III which are in the positive octant. The points of the set (b) are the points on the straight lines in the positive octant originating from curve II.

All values of $\bar{K}_1$, $\bar{K}_2$, $\bar{K}_3$ less than the values determined by (27), (28) and (29) determine stable equilibrium. All values greater than these give unstable equilibrium.

We may note that the equilibrium is stable for

$$0 < \bar{K}_1 < \infty, \quad 0 < \bar{K}_2 < \pi/2, \quad 0 < \bar{K}_3 < \pi/4. \quad \ldots(30)$$

There are in addition other parametric values for which the equilibrium is stable due to the fact that the curves II and III are concave upwards on the $\bar{K}_1$–$\bar{K}_2$ and $\bar{K}_1$–$\bar{K}_3$ phase planes.

4. The Fourth Model

We consider the logistic model with distributed time delay

$$\frac{dN}{dt} = N(t)\left[a - b\int_0^\infty N(t-s)\,k(s)\,d(s)\right];\quad \int_0^\infty k(s)\,ds = 1. \qquad ...(31)$$

The characteristic equation comes out to be

$$\lambda + ak^*(\lambda) = 0;\quad k^*(\lambda) = \int_0^\infty e^{-\lambda u}k(u)\,du. \qquad ...(32)$$

Considering the linear chain model for which

$$k(u) = \frac{e^{-\alpha u}u^{q-1}\alpha^q}{\pi(q)};\quad k^*(\lambda) = \left(\frac{\alpha}{\alpha+\lambda}\right)^q \qquad ...(33)$$

we get

$$\lambda + a\left(\frac{\alpha}{\alpha+\lambda}\right)^q = 0. \qquad ...(34)$$

If it has roots $\pm is$, (34) gives

$$\cos^q\beta\cos q\beta = 0,\quad \alpha\tan\beta + a\sin q\beta\cos^q\beta = 0 \qquad ...(35)$$

where

$$a = r\cos\beta,\quad s = r\sin\beta \qquad ...(36)$$

so that

$$a = (\alpha\tan\pi/2q)/(\cos\pi/2q)^q. \qquad ...(37)$$

For values of a less than that given by (37), the equilibrium is stable and for values greater than this, the equilibrium is unstable.

If $\alpha = q$, we get

$$\lim_{q\to\infty} a = \lim_{q\to\infty}\frac{q\tan\pi/2q}{(\cos\pi/2q)^q} = \pi/2 \qquad ...(38)$$

which is the critical value obtained for the first model. In this limiting case, the distributed delay model reduces to the discrete delay model.

5. The Fifth Model

We consider the logistic model with both non-delay and distributed time delay terms so that

$$\frac{dN}{dt} = N(t)\left[a - bN(t) - c\int_0^\infty N(t-u)\,k(u)\,du\right]. \qquad ...(39)$$

The characteristic equation comes out to be

$$\lambda + K_1 + K_2\left(\frac{\alpha}{\alpha+\lambda}\right)^q = 0. \qquad ...(40)$$

If

$$\lambda = is, \quad a = r\cos\beta, \quad s = r\sin\beta \qquad ...(41)$$

we get

$$K_1 + K_2\cos^q\beta\cos q\beta = 0, \quad \alpha\tan\beta - K_2\cos^q\beta\sin q\beta = 0 \qquad ...(42)$$

or

$$\frac{K_1}{\alpha} = -\frac{\tan\beta}{\tan q\beta}, \quad \frac{K_2}{\alpha} = \frac{\tan\beta}{\cos^q\beta\sin q\beta}. \qquad ...(43)$$

We can draw the graph between K_1/α and $K_2/\alpha\cos\beta$ values from $\pi/2q$ to π/q. For each value of q, the region below the curve corresponds to stable equilibrium and the region above the curve corresponds to unstable equilibrium.

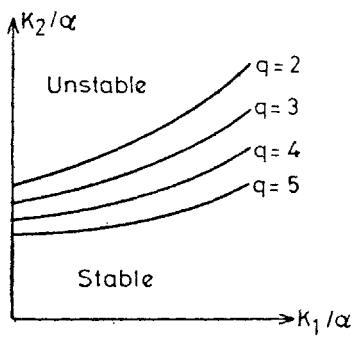

Fig. 7.

The region of stable equilibrium decreases as q increases, but it always includes the region $K_2 = K_1$.

6. The Sixth Model

Here we allow the species of the first model to diffuse in a finite domain, say a rectangular parallelopiped with edges of lengths a, b, c in such a way that there is no flow across the bounding surfaces. If D is the diffusion coefficient, the model is

$$\frac{\partial N}{\partial t} = N(x, y, z, t)\,[a - bN(x, y, z, t-1)] + D\left[\frac{\partial^2 N}{\partial x^2} + \frac{\partial^2 N}{\partial y^2} + \frac{\partial^2 N}{\partial z^2}\right] \quad \ldots(44)$$

Substituting

$$N(x, y, z, t) = \frac{a}{b} + u(x, y, z, t) \quad \ldots(45)$$

in (44) and linearising, we get

$$\frac{\partial u}{\partial t} = -au(x, y, z, t-1) + D\left(\frac{\partial^2 u}{\partial x^2} + \frac{\partial^2 u}{\partial y^2} + \frac{\partial^2 u}{\partial z^2}\right) \quad \ldots(46)$$

with boundary conditions

$$\frac{\partial u}{\partial x} = 0 \text{ at } x = 0, a; \quad \frac{\partial u}{\partial y} = 0 \text{ at } y = 0, b; \quad \frac{\partial u}{\partial z} = 0 \text{ at } z = 0, c. \quad \ldots(47)$$

Trying the solution

$$u(x, y, z, t) = e^{\lambda t} \sum_p \sum_n \sum_m A_{mnp} \cos\frac{m\pi x}{a} \cos\frac{n\pi y}{b} \cos\frac{p\pi z}{c} \quad \ldots(48)$$

which identically satisfies the boundary conditions, we get

$$\lambda + ae^{-\lambda} + D\sigma^2 = 0, \; \sigma^2 = \left(\frac{m^2}{a^2} + \frac{n^2}{b^2} + \frac{p^2}{c^2}\right)\pi^2. \quad \ldots(49)$$

This is the same form as (14) and Fig. 5 applies to it using (14), it shows that an equilibrium position which is stable in the absence of diffusion will continue to remain stable in the presence of diffusion and so diffusive instability cannot arise in this case.

7. The Seventh Model

Here we introduce diffusion effect in the third model to get the characteristic equation

$$\lambda + K_1 + K_2 e^{-\lambda} + D\sigma^2 = 0. \quad \ldots(50)$$

For purely imaginary roots, this gives

$$s - K_2 \sin s = 0, \; K_1 + K_2 \cos s + D\sigma^2 = 0. \quad \ldots(51)$$

Eliminating s, we get a ruled surface with equation of the form

$$z = f(x + y) \quad \ldots(52)$$

for which

$$\frac{\partial^2 z}{\partial x^2}\frac{\partial^2 z}{\partial y^2} - \left(\frac{\partial^2 z}{\partial x \partial y}\right)^2 = 0 \quad \ldots(53)$$

so that the surface is a developable surface which divides the positive octant into stable and unstable regions. In fact if $K_2 = f(K_1)$ is the equation of curve I of Fig. 5, then $K_2 = f(K_1 + D\sigma^2)$ is the equation of the ruled surface here.

For the distributed time delay, we get

$$\lambda + K_1 + K_2\left(\frac{\alpha}{\alpha + \lambda}\right)^q + D\sigma^2 = 0 \qquad \ldots(54)$$

and again we get a ruled developable surface separating regions of stable and unstable equilibrium in the three dimensional phase space.

We can introduce diffusion in each of the models discussed above and decide whether diffusive instability can arise.

8. The Eighth Model

Here we consider predator-prey models with discrete time delays

$$\frac{dN_1}{dt} = N_1(t)\,[a_1 - \alpha_1 N_2(t - k)] \qquad \ldots(55)$$

$$\frac{dN_2}{dt} = N_2(t)\,[-a_2 + \alpha_2 N_2(t - 1)]. \qquad \ldots(56)$$

The characteristic equation for this model is

$$\lambda^2 + a_1 a_2 e^{-\lambda(1+k)} = 0 \quad \text{or} \quad z^2 + be^{-z} = 0 \qquad \ldots(57)$$

where

$$z = \lambda(1 + k),\ b = a_1 a_2 (1 + k)^2. \qquad \ldots(58)$$

If $z = \pm is$ are roots of (57), then

$$-s^2 + b\cos s = 0,\ b\sin s = 0 \qquad \ldots(59)$$

or

$$s = 2n\pi,\ b = 4n^2\pi^2. \qquad \ldots(60)$$

If $z = r \pm is$ are roots of (57), then

$$r^2 - s^2 + be^{-r}\cos s = 0,\ 2rs - be^{-r}\sin s = 0 \qquad \ldots(61)$$

or

$$r = s\tan \tfrac{1}{2}s,\ s^2 = b\exp(-s\tan \tfrac{1}{2}s)\cos^2 \tfrac{1}{2}s. \qquad \ldots(62)$$

The solutions of the second equation of (62) are given by the points of intersection of

$$y = x^2,\ y = b\exp(-x\tan \tfrac{1}{2}\pi)\cos^2 \tfrac{1}{2}x. \qquad \ldots(63)$$

Both curves are symmetrical about OY. The second curve has asymptotics at $x = \pm\pi, \pm 3\pi, \pm 5\pi, \ldots$.

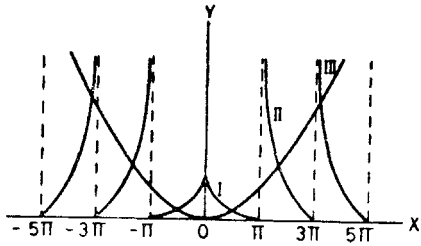

FIG. 8.

There is always a point of intersection between 0 and π and for this $r > 0$. If $b > 4\pi^2$, there is another point of intersection and for this also $r > 0$.

If $b > 16\pi^2$, there is a third point of intersection and for this also $r > 0$ and so on. Thus for all values of a_1, a_2, k, there is at least one pair of complex roots with $r > 0$ and if b is large, there may be more than one such pair. Thus for all values of a_1, a_2, k, the equilibrium position is unstable. Now from (62)

$$\frac{dr}{ds} = \tfrac{1}{2}s \sec^2 \tfrac{1}{2}s + \tan \tfrac{1}{2}s = \frac{s-1}{2} \sec^2 \tfrac{1}{2}s + \tfrac{1}{2}(1 + \tan \tfrac{1}{2}s)^2 \qquad \ldots(64)$$

so that $dr/ds > 0$ for all s. Again

$$\frac{db}{dr} = \tfrac{1}{2} \exp(s \tan \tfrac{1}{2}s)\, s \sec^2 \tfrac{1}{2}s\, [s^2 + (s \tan \tfrac{1}{2}s + 2)^2] \qquad \ldots(65)$$

so that $db/ds > 0$ for all s; so that

$$\frac{dr}{db} > 0 \qquad \ldots(66)$$

so that each root increases as b increases.

Each of the branches I, II, III, ... of Fig. 8 determines a root.

	s	$\pi/10$	$2\pi/10$	$3\pi/10$	$4\pi/10$	$5\pi/10$	$6\pi/17$	
I	r	0.049	0.204	0.480	0.913	1.571	2.594	
	b	0.106	0.535	1.808	6.012	23.738	137.691	
	r	$11\pi/10$	$13\pi/10$	$15\pi/10$	$17\pi/10$	$19\pi/10$	$20\pi/10$	$22\pi/10$
II	s	−21.819	−8.015	−4.712	−2.721	−0.945	0	2.246
	b	0	0.027	0.395	2.364	14.190	39.478	498.910
	r	$32\pi/10$	$35\pi/10$	$37\pi/10$	$38\pi/10$	$39\pi/10$	$40\pi/10$	
III	s	−30.940	−10.996	−5.992	−3.879	−1.941	0	
	b	0	0.004	0.456	3.257	22.101	157.933	

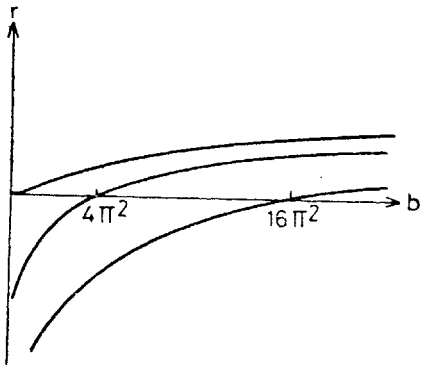

FIG. 9.

The signs of the real parts of the roots are given in Fig. 10.

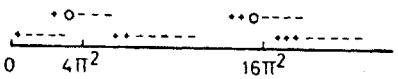

FIG. 10.

9. CONCLUDING REMARKS

Models with time delays have been discussed in Cushing (1977) and Macdonald (1978) while models with diffusion have been discussed in Murray (1977) and Fife (1976). Recently Kapur (1979a, 1980d) has discussed some of these models.

In the present paper, we have discussed the stability of eight models with time delays. In each case we get an algebraic or transcendental characteristic equation and we have to find the signs of the real parts of its roots. We find the values of the parameters for which this equation has purely imaginary roots. Here the real part of a root may change sign as the parameters change slightly. If a is a parameter, we may find $\delta r/\delta a$ at each of these points. In the first model $\delta r/\delta a$ was positive at all points and in particular at points where $r = 0$ so that at each of these points one pair of complex roots changes the sign of its real part from negative to positive. The same situation was true for the eighth model.

It is obvious that the methods used in the present paper can be used effectively with many more models with time delays.

REFERENCES

Cushing, J. M. (1977). Integrodifferential Equations and Delay Models on Population Dynamics. Springer Verlag, New York.

Fife, P. C. (1976). Pattern formation in reacting and diffusing systems. *J. Chem. Phys.*, **64**, 554-64.

Kapur, J. N. (1979a). Time delay predator-prey models. *J. Math. Phys. Sci.*, (to appear).

——————— (1979b). Predator-prey models with discrete time lags. *Natn. Acad. Sci. Letters*, **2**, 273–75.

——————— (1980a). On the stability analysis of a population model with time lag. *Indian J. Math.*, (to appear).

——————— (1980b). Delay-differential and integro-differential equation of population dynamics. *J. Math. Phys. Sci.*, (to appear).

——————— (1980c). A note on predator-prey model with discrete time lag. *Natn. Acad. Sci. Letters*, **3**, No. 3.

——————— (1980d). Diffusive instability for diffusion-reaction systems in female domains. *J. Math. Phys. Sci.*, (to appear).

Macdonald, N. (1978). Time Lags in Biological Models. Springer Verlag, New York.

Murray, J. D. (1977). Lectures on Non-linear Differential Equations of Models of Biology. Clarendon Press, Oxford.